International Journal of Control and Automation
Vol.8, No.4 (2015), pp.63-74
http://dx.doi.org/10.14257/ijca.2015.8.4.08

An Enhanced Droop Control Scheme for Islanded Microgrids

Lianqing Zheng, Chen Zhuang, Jian Zhang and Xiong Du

State Key Laboratory of Power Transmission Equipment & System Security and New Technology, Chongqing University, Chongqing, China
zhuangchen921@126.com

Abstract

Due to the line impedance impact on islanded low-voltage microgrids, traditional droop control cannot guarantee the proper power sharing between distributed generation (DG) units. In the meanwhile, droop control would cause voltage and frequency deviation, which will influence the power quality of customers. This paper proposed an enhanced droop control scheme with autonomous frequency restoration control. Reactive power sharing problem is solved by adding a redesigned virtual impedance and voltage compensation loop, which ensures PCC voltage in nominal range. To the problem of frequency deviation, autonomous frequency restoration loop is added. Small signal model of frequency control is established to analyze the stability. In circumstance of frequent load switching, the frequency can properly restore to nominal value, with smooth and stable transient process. The simulation results demonstrate the effectiveness of the proposed control strategy.

Keywords: *Droop control, virtual impedance, frequency restoration, small signal analysis*

1. Introduction

Microgrids are small power grids comprising multiple distributed generations (DGs), loads, power electronics converters, energy storage systems and telecommunications that not only can operate in grid-connected mode but also in islanded mode [1]. The flexible control of multiple DGs strengthen its reliability and power quality, in the meantime eliminate the impact of unstable power supply to our grids [2].

The main goals to ensure stable and efficient operation are frequency and voltage regulation, power control, synchronization, energy management, and economic optimization [3-6]. When in islanded mode, droop control is adopted. Based on the relationship between active power and frequency, reactive power and voltage, inverters can control the output to realize proper power sharing [7-9].

But in fact droop control strategy is usually unstable due to the power coupling, consequently its sharing is inaccurate. Some scholars propose to add a virtual impedance into the control loop so that the output impedance of DGs could be inductive [10-12]. Proper design of the control is inevitable. Small signal model considering virtual impedance is analyzed in [12], but the influence of changing loads has not been taken into consideration. To the impact of line impedance, an accurate power sharing method is proposed in [13].

In the other hand, droop control is based on the frequency and voltage deviation to realize the power sharing strategy. But this kind of deviation could have an impact on the stability of microgrids. So [1] and [4] discussed an autonomous restoration control to restore the frequency and voltage. So the control stability and dynamic performance is to be analyzed.

By analyzing the conventional droop control scheme used in islanded microgrids, this paper proposed an enhanced droop control strategy with accurate power sharing control

ISSN: 2005-4297 IJCA

and frequency autonomous restoration. In this scheme, a well-designed voltage compensation unit is added; virtual impedance is renovated with new characteristics. The small signal model of frequency control is established. By analyzing the obtained eigenvalues, we can properly adjust the PI control parameters. Finally, simulation results are provided to verify the proposed method.

2. Microgrid Conventional Droop Control

Conventional *P–f* and *Q–V* droop control are illustrated in Figure 1. The output voltage of two DGs are $V_1\angle\theta_1$ and $V_2\angle\theta_2$. $V_p\angle\theta_p$ represents the voltage at point of common coupling (PCC). So the power flow through the line impedance ($Z_1=R_1+jX_1$, $Z_2=R_2+jX_2$) is as

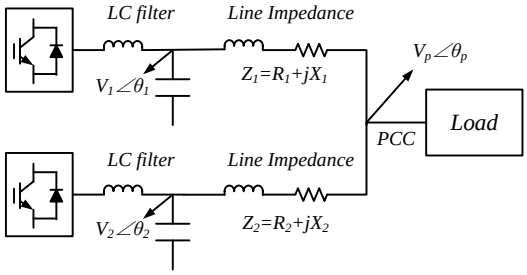

Figure 1. Simplified Circuit of the Microgrid

$$P_x = \frac{V_x}{R_x^2 + X_x^2}[R_x\left(V_x - V_p\cos\theta_{xp}\right) + X_x V_p \sin\theta_{xp}] \tag{1}$$

$$Q_x = \frac{V_x}{R_x^2 + X_x^2}[-R_x V_p \sin\theta_{xp} + X_x\left(V_x - V_p\cos\theta_{xp}\right)] \tag{2}$$

where *x=1, 2* represents two DG branches, θ_{xp} is the phase angle difference between output voltage V_x and PCC voltage V_p. If the line inductor is much bigger than the resistor, the above power flow equation can be simplified like this

$$P_x = \frac{V_x V_p}{X_x}\sin\theta_{xp} \tag{3}$$

$$Q_x = \frac{V_x(V_x - V_p\cos\theta_{xp})}{X_x} \tag{4}$$

From (3) and (4), the relationship of *P-f* and *Q-V* can be derived. As a result, (5) and (6) are obtained to regulate the output voltage and frequency as follows

$$f_n = f^* - m(P - P_n) \tag{5}$$

$$V_n = V^* - n(Q - Q_n) \tag{6}$$

where *m* is the frequency droop coefficient; *n* is the voltage droop coefficient; f^* is the nominal frequency; V^* is the nominal phase voltage amplitude.

At present, the triple-loop feedback control structure is the main scheme used in droop controller. Power control loop is mentioned above. After that voltage and frequency reference signal will be calculated; voltage and current double-loop control is adopted here. Inner current loop is aimed at promoting the controller performance, while outer loop is mainly used to generate reference signal for inner loop to regulate voltage [14-15].

Figure 2 shows the above control structure, in which C_f and L_f represent filter capacitor and inductor, ω is the reference angular frequency, and V_{od}^* and V_{oq}^* are *d-q* components of reference voltage respectively. PI control in voltage loop can stabilize output voltage, and proportion control in current loop will improve the response speed.

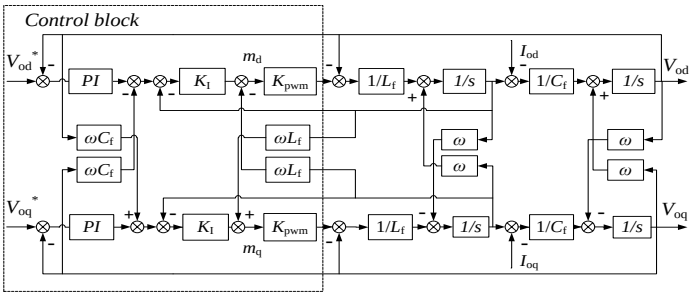

Figure 2. Double-loop Control Structure

3. Enhanced Droop Control Scheme

3.1. Virtual Impedance Control

For the low-voltage microgrid, line impedance is mainly resistive. Refer to (3) and (4), this kind of control will be effected by the coupling of active and reactive power. As a result, power sharing is inaccurate and the system stability is poor. In order to eliminate its impact on our controller, virtual impedance is added here with advantages like power decoupling and circulating current restraining.

Figure 3 is the entire control block diagram of the islanded microgrid inverters. To emulate the effect of real inductor, the control loop generates V_{vzd} and V_{vzq} as emendation signal, which are in fact voltage drop of the virtual impedance. A well-designed approach is proposed here to reach accurate sharing of power and good performance of the droop controller.

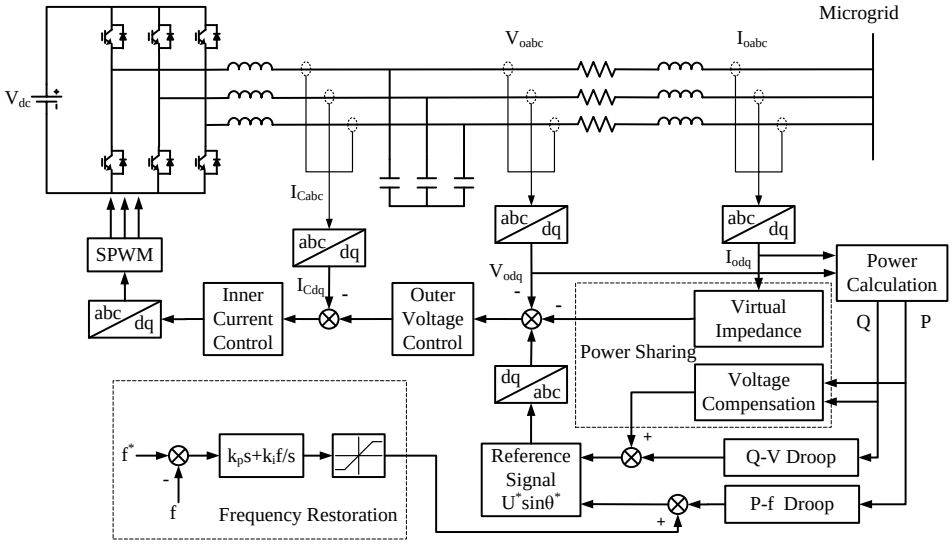

Figure 3. Control Block Diagram of the DG Inverter

As shown in Figure 2, the transfer function of the double-loop control system is as follows

$$V_{odq} = \frac{k_2 k_{pwm} C_f s^2 + k_{1p} k_2 k_{pwm} s + k_{1i} k_2 k_{pwm}}{As^3 + Bs^2 + Cs + D} V_{odq}^* - \frac{L_f s^2}{As^3 + Bs^2 + Cs + D} I_{odq} \quad (7)$$

where $A = C_f L_f$, $B = k_2 k_{pwm} C_f$, $C = 1 + k_{1p} k_2 k_{pwm}$, $D = k_{1i} k_2 k_{pwm}$

Thus the output voltage can be expressed as

$$V_{odq} = G(s) V_{odq}^* - Z_{on}(s) I_{odq} \quad (8)$$

where $G(s)$ is the voltage closed-loop transfer function, $Z_o(s)$ is the equivalent output impedance of inverters.

As seen in (8), it represents the equivalent Thevenin circuit of the closed-loop system. $G(s)V_{odq}^*$ is the equivalent voltage source, and $Z_o(s)$ is the equivalent source impedance. As a result, the virtual impedance control loop can be added to change the output impedance.

The virtual impedance is designed to have an inductive behavior for the low-frequency components and a resistive behavior for the high-frequency components. Benefit from this design, the total harmonic distortion is in desirable range and the power sharing is ensured. To realize this kind of demand, the following equation is designed

$$V_{vzd} = -j\omega L_{vz} I_{ofq} + I_{ohd} R_{vz} \quad (9)$$

$$V_{vzq} = j\omega L_{vz} I_{ofd} + I_{ohq} R_{vz} \quad (10)$$

where I_{ofd}, I_{ofq}, I_{ohd}, I_{ohq} represent the fundamental and high-order harmonic component of the output current respectively.

Clarke and Park transformation is applied to the output current to get its *d-q* component. Then as shown in (11), low-pass filter (LPF) is used for fundamental component extraction. After a simple calculation in (12), the high-order harmonic component is also extracted.

$$I_{of,dq} = \frac{\omega_c}{s + \omega_c} I_{om,dq} \quad (11)$$

$$I_{oh,dq} = I_{om,dq} - I_{of,dq} \quad (12)$$

where ω_c is the cut-off frequency of LPF, $I_{om,dq}$ represents the measured output current.

Figure 4 shows the control scheme of virtual impedance, which is proposed to avoid the differentiation by transforming sL_{vz} as $j\omega L_{vz}$, where ω is the system angular frequency. Voltage drop calculation of virtual impedance is realized in *d-q* frame.

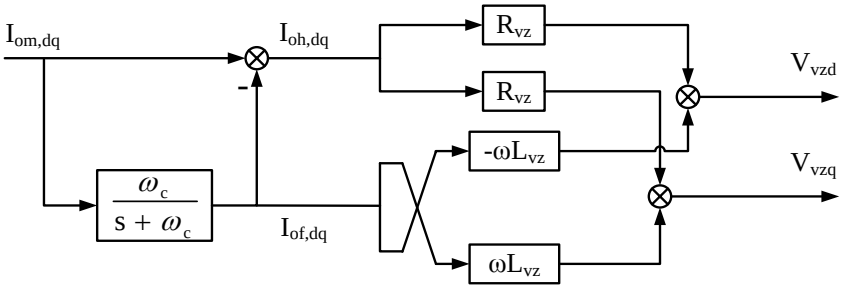

Figure 4. Block Diagram of Virtual Impedance Loop

3.2. Voltage Compensation and Reactive Power Sharing

For the inaccurate reactive power sharing problem, power coupling is the main reason. So far, droop control discussion is usually based on the assumption of strict *P-f* and *Q-V* relationship. But in low-voltage microgrid, *R/X* of line impedance is relatively high. So voltage drop caused by the line and virtual impedance will have an impact on the PCC voltage.

This paper proposed a simple and effective voltage compensation method to offset the influence of line and virtual impedance. Refer to power system analysis knowledge, the voltage drop of line impedance is as follows

$$\Delta V = \frac{PR + QX}{V} \tag{13}$$

where ΔV is the voltage amplitude difference between two ends of the transmission line.

Based on (13), voltage compensation loop is derived. Measured output active and reactive power are used in feedback regulation to promote the power sharing performance. Hence new *Q-V* droop control is as follows

$$V_n = V^* + V_{comp} - n(Q - Q_n) \tag{14}$$

where V_{comp} is the voltage compensation loop

$$V_{comp} = \frac{PR_L + Q\left(X_L + X_{vz}\right)}{V_o} \tag{15}$$

X_{vz} is virtual reactance; V_o is output voltage of inverters; P is the output active power; Q is the output reactive power. The block diagram of voltage compensation is shown in Figure 5.

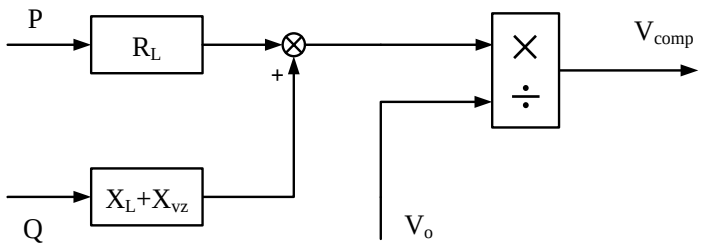

Figure 5. Block Diagram of Voltage Compensation

It is worth noting that if there are local loads at the DG unit location, power of local loads should be taken out like this $P = P_o - P_b$, $Q = Q_o - Q_b$. That is to say only the power flowing through the transmission line should be considered in the compensation. The effect of this control design will be verified in Section 4.

3.3. Frequency Autonomous Control

The voltage and frequency deviation in droop control would decrease the system stability. To voltage, traditional regulation method could also be used in microgrids, such as reactive power compensation, transformer regulation, etc. But system frequency is only determined by DG inverters. So this paper proposes an autonomous restoration method to ensure the system frequency in desirable range.

In traditional power grid, the aforementioned frequency deviation can be regulated through secondary frequency control [16], which may also be achieved in microgrids. Normally in low-voltage and small-capacity power grid, frequency tolerance is 50±0.5Hz. The frequency restoration control is introduced based on a slow PI control with a dead band of ±20mHz. That is to say PI control is activated only in case of the error exceeding defined range.

In the proposed method, measured frequency is compared with nominal value to get an error signal, which will pass through the PI controller to generate restoring signal f_{res} as

$$f_{res} = k_{fp}\left(f_{sys}^{*} - f_{DG}\right) + k_{fi}\int\left(f_{sys}^{*} - f_{DG}\right)dt \tag{16}$$

k_{fp} and k_{fi} are the PI parameters; f_{sys}^{*} is the nominal frequency; f_{DG} is the measured frequency. Thus final restoring signal f_{res} is generated to compensate the deviation.

As shown in Figure 6, the power capacity and *P-f* droop coefficient of two DGs are different. Under this circumstance the restoration is still effective to properly control the frequency.

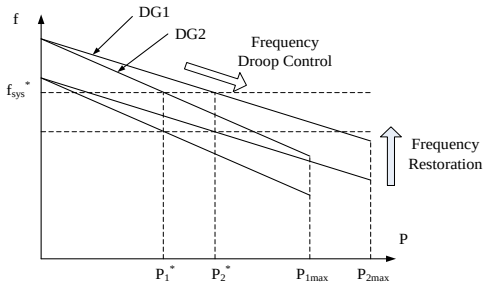

Figure 6. Frequency Droop and Restoration Curve

To analyze the system stability and adjust the PI parameters, a small signal model of frequency control has been established.

From (3) the small signal equation of inductive-line power transmission can be derived

$$\Delta p_{DG} = G_P \Delta\theta_{xp} \tag{17}$$

where G_p is the transfer function. It can be expressed as follows

$$G_p = \frac{V_{DG}V_p}{X_L}\cos\theta_{xp} \tag{18}$$

V_{DG} is the output voltage of inverters; V_P is the voltage in PCC; X_L is the impedance of transmission line; θ_{xp} represents the power angle.

Normally Δp_{DG} would pass through a low-pass filter with cut-off frequency ω_c to get the power signal used in droop calculation. So its small signal is as

$$\Delta P_{DG} = \frac{\omega_c}{s+\omega_c}\Delta p_{DG} \tag{19}$$

According to (5), the small signal of *P-f* droop control is derived as

$$\Delta\omega_{DG} = -G_{droop}\Delta P_{DG} \tag{20}$$

among which G_{droop} is the droop coefficient.

$$G_{droop} = m \tag{21}$$

Refer to the frequency restoration control equation (16), its small signal is

$$\Delta\omega_{res} = -G_{res}\Delta\omega_{DG} \tag{22}$$

where G_{res} is the restoration transfer function as follows

$$G_{res} = k_{fp} + \frac{k_{fi}}{s} \tag{23}$$

Moreover, with restoration control the equation of $\Delta\omega_{DG}$ should be changed from (19) to

$$\Delta\omega_{DG} = -G_{droop}\Delta P_{DG} + \Delta\omega_{res} \tag{24}$$

Considering that $\Delta\theta_{xp} = (1/s) \cdot \Delta\omega_{DG}$, (17), (19), (20), (22) and (24) can be manipulated to get

$$\Delta\omega_{DG} = -G_{droop}\frac{\omega_c}{s+\omega_c}G_p\frac{1}{s}\Delta\omega_{DG} - G_{res}\Delta\omega_{DG} \tag{25}$$

the closed-loop characteristic equation of the frequency control can be obtained as

$$\Delta = 1 + G_{res} + G_{droop} \times G_P \times \frac{\omega_c}{s+\omega_c} \times \frac{1}{s} \tag{26}$$

By analyzing the eigenvalues in (26), the performance of control system can be indicated. To ensure stable operation, all eigenvalues should be in left of the imaginary axis.

The performance of the whole frequency control block with increasing k_{fp} and k_{fi} are shown in Figure 7(a) and (b) respectively. As illustrated, it is a two-order system with two poles being both the dominate poles λ_1 and λ_2. Its dynamic performance is mainly determined by choosing the value of k_{fp} and k_{fi}.

In Figure 7(a), root locus of λ_1 and λ_2 are sensitive to change of control parameter k_{fp}. When k_{fp} increase, the real and imaginary part both decrease which is not desirable. In order to ensure its stability, k_{fp} is selected as 0.01 with enough real and imaginary value.

As shown in Figure 7(b), root locus of λ_1 and λ_2 are sensitive to change of k_{fi}, which mainly influence the real part. Considering appropriate inertia of restoration control and stability of the system, k_{fi} is selected as 5 compared with k_{ui} value 200. In this case, power sharing of frequency droop is ensured and restoration is also realized with relatively greater inertia.

Through the analyzing of the small signal and its root locus, PI parameters k_{fp} and k_{fi} are well-designed. The system shows satisfied performance and dynamic stability which will be demonstrated in the next section.

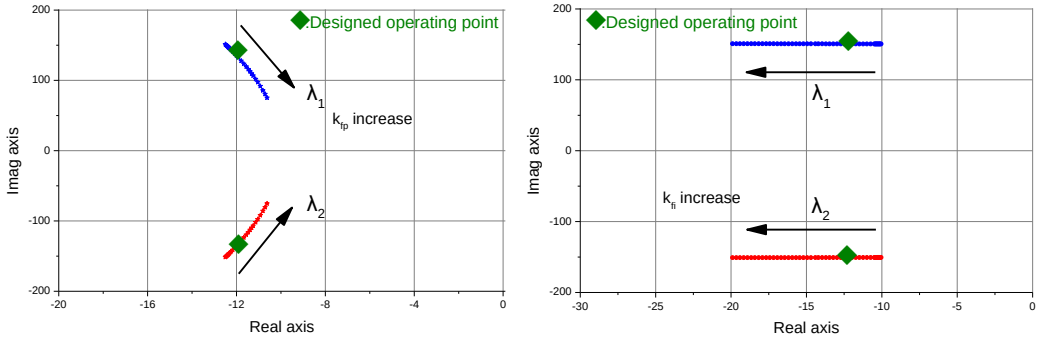

(a) Root locus diagram with increasing k_{fp} (b) Root locus diagram with increasing k_{fi}

Figure 7. Root Locus of Frequency Control

4. Simulation Result

Islanded microgrid model with two parallel DG inverters has been established in Matlab/Simulink, adopting control scheme proposed in this paper to verify its performance.

Table 1. DG System Parameters

Parameter		Value
DG and inverter parameters	P_n	16kW, 24kW
	Q_n	4.0kVar, 4.0kVar
	L_f/R_f	1.3mH/0.01Ω
	C_f	1200μF
	R_{line}/L_{line}	0.15Ω/2mH
	R_{vz}/L_{vz}	0.33Ω/4mH
	Nomial V/f	220V(RMS L-L)/50Hz
Control block parameters	m	0.0003142rad/W
	n	0.000547V/Var
	k_{up}	5.328
	k_{ui}	216
	k_{fp}	0.01
	k_{fi}	5
	ω_c	20Hz

Simulation results of power sharing is shown in Figure 8. Before t=6.0s, load power is P_{L1}=40kW, Q_{L1}=8kVar. The microgrid is originally operated with conventional droop control. As seen, active power are both the nominal value 16kW and 24kW, while reactive power sharing is inaccurate. Reactive power of DG_1 is 1kVar more than that of DG_2. At t=3.0s, virtual impedance and voltage compensation is activated. As expected, Q_1 and Q_2 both reach.

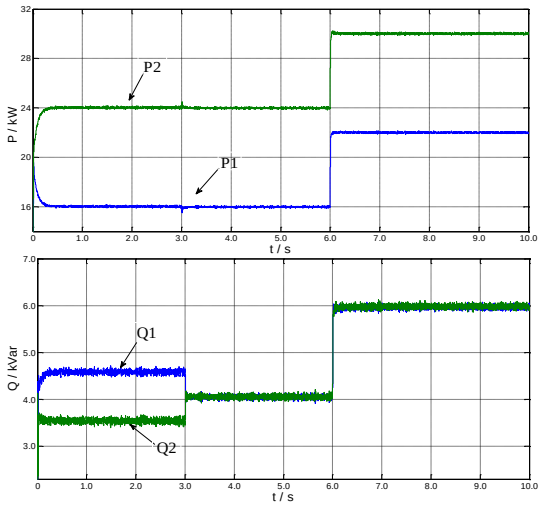

(a) Active power sharing of DG_1 and DG_2 (b) Reactive power sharing of DG_1 and DG_2

Figure 8. Power Sharing with Virtual Impedance and Voltage Compensation

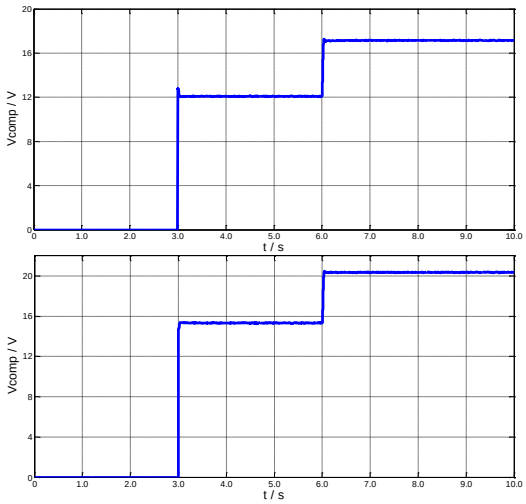

(a) Signal of DG_1 (b) Signal of DG_2

Figure 9. Voltage Compensation Output Signal

the nominal value 4.0kVar with fast transient process and little influence on active power. At t=6.0s, the load power increase to P_{L2}=52kW, Q_{L2}=12kVar. Reactive power sharing control still performs well. Figure 9 shows that the voltage compensation signal of two DGs has fast and accurate response to changing load.

In the next step, frequency restoration control is added. Change of active load power is shown in Figure 10(b), which indicates the rise and drop of frequency. At t=1.0s, when frequency starts to droop, the restoration control is activated immediately. After about 2.0s, frequency restores to 50Hz autonomously, as shown in Figure 10(a). At t=4.0s and t=7.0s, it is the same case with desirable dynamic performance and restoration effect. In Figure 10(c), reactive power sharing still performs well after the adding of restoration control.

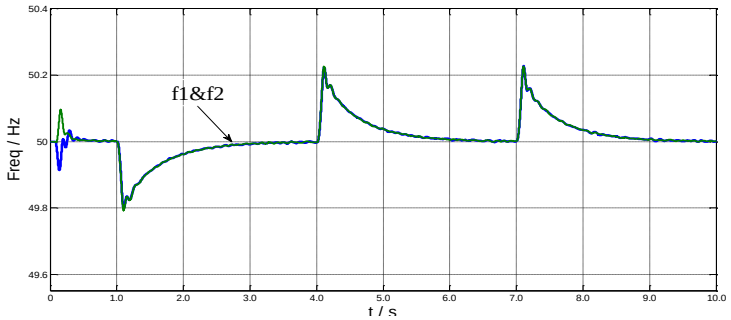

(a) Frequency of DG_1 and DG_2

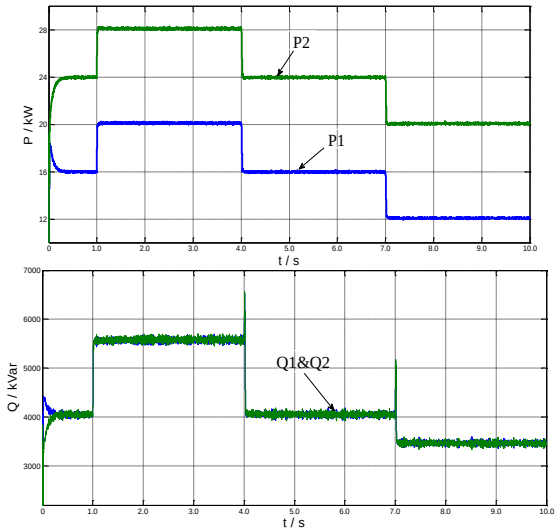

(b) Active power of DG_1 and DG_2 (c) Reactive power of DG_1 and DG_2

Figure 10. Frequency and Power of DGs while Load Changes

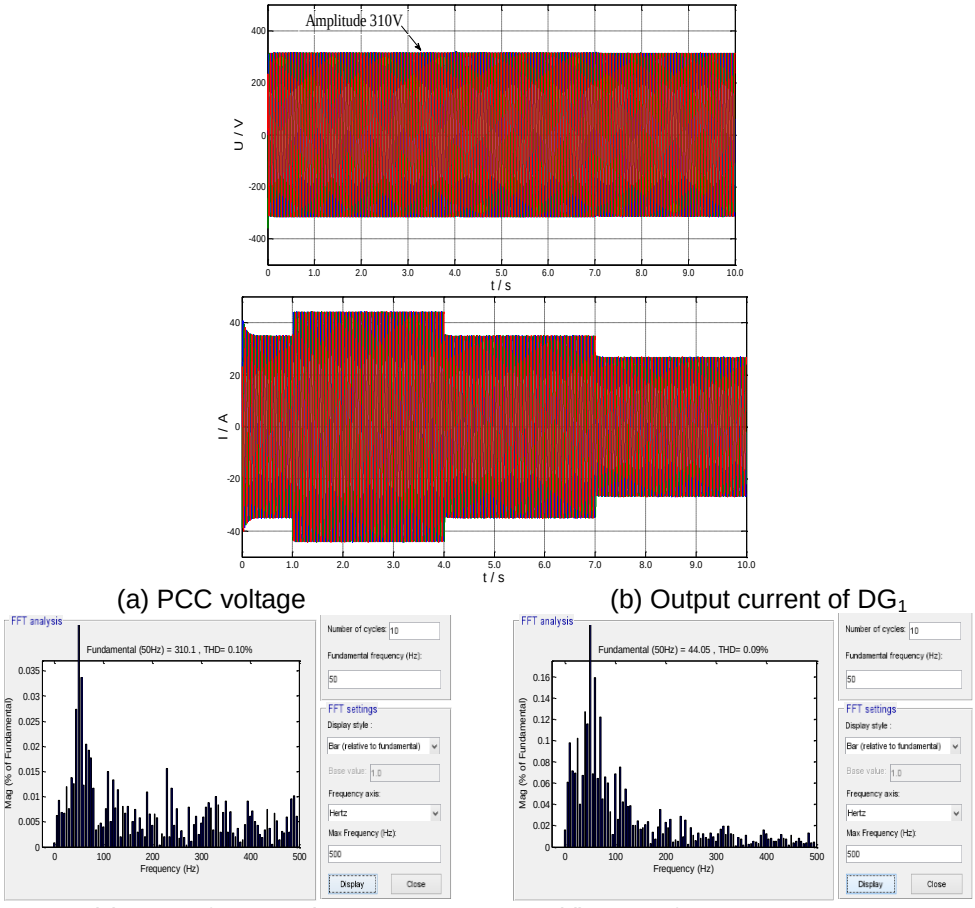

(a) PCC voltage (b) Output current of DG_1

(c) THD of PCC voltage (d) THD of DG_1 output current

Figure 11. System Voltage and Current Waveform

Figure 11(a) is the voltage waveform at PCC. As can be seen, the amplitude keeps around the nominal value 310V which demonstrates that voltage can be stable without extra restoration. Figure 11(b) is the waveform of DG_1 output current with smooth transient process when load changes or control is activated. Meanwhile the current

waveform of DG_2 has the same performance. FFT analysis is applied to get Total Harmonic Distortion (THD) of PCC voltage and DG_1 output current from 3.0s to 4.0s. Both THD are maintained in relatively low range shown in Fig 11(c), (d).

5. Conclusion

This paper has introduced an enhanced droop control scheme with accurate power sharing and frequency restoration strategy. In this method, a well-designed virtual impedance and voltage compensation loop are added to the conventional droop control scheme, thus improving the power sharing performance even two DGs have different power capacity. Through the resistive behavior for the high-frequency components in virtual impedance loop, THD of both voltage and current keep in low range. Furthermore, frequency deviation caused by *Q-V* droop is solved by introducing a PI control loop as autonomous restoration control. The small signal model of frequency control is built to analyze the system stability, choosing desirable PI parameters. Smooth frequency restoration is ensured under circumstance of frequent load change. Simulation results demonstrate the feasibility and effectiveness of the proposed method.

Acknowledgements

This work was supported by National Natural Science Foundation of China (Project No. 51277191) and the Fundamental Research Funds for the Central Universities (Project No. CDJXS12151106).

References

[1] J. M. Guerrero, J. C. Vasquez, J. Matas, L. G. Vicuna and M. Castilla, " Hierarchical control of droop-controlled AC and DC microgrids– A general approach toward standardization" , IEEE Trans on Industrial Electronics, vol. 58, no. 1, **(2011)**, pp. 158-172.
[2] S. Shi, Z. Lu, Y. Min and Y. Wang, " Analysis on Frequency Characteristics of Islanded Microgrid" , Automation of Power Systems, vol. 35, no. 9, **(2011)**, pp. 36-41.
[3] M. C. Chandorkar, D. M. Divan and R. Adapa, " Control of parallel connected inverters in standalone AC supply systems" , IEEE Trans on Industrial Applications, vol. 29, no. 1, **(1993)**, pp. 136-143.
[4] Y. A. R. I. Mohamed and A. A. Radwan, " Hierarchical control system for robust microgrid operation and seamless mode transfer in active distribution systems" . IEEE Trans on Smart Grid, vol. 2, no. 2, **(2011)**, pp. 352-362.
[5] J. H. Kim, J. M. Guerrero, P. Rodriguez, R. Teodorescu and K. Nam, " Mode adaptive droop control with virtual output impedances for an inverter-based flexible AC microgrid" , IEEE Trans on Power Electronics, vol. 26, no. 3, **(2011)**, pp. 689-701.
[6] F. Katiraei, M. R. Iravani and P. W. Lehn, " Microgrid autonomous operation during and subsequent to islanding process" , IEEE Trans on Power Delivery, vol. 20, no. 1, **(2005)**, pp. 248-257.
[7] C. Wang, Z. Xiao and S. Wang, " Multiple feedback loop control scheme for inverters of the microsource in microgrids" , Transactions of China Electrotechnical Society, vol. 24, no. 2, **(2009)**, pp. 100-107.
[8] J. Xu, J. Li and M. Zhang, " Control method of voltage support for microgrid" , Power System Technology, vol. 36, no. 9, **(2012)**, pp. 36-42.
[9] F. Li and M. Wu, " An improved control strategy of load distribution in an autonomous microgrid" , Proceedings of the Chinese Society of Electrical Engineering, vol. 31, no. 13, **(2011)**, pp. 18-25.
[10] J. Cheng, S. Li, Z. Wu and J. Chen, " Analysis of Power Decoupling Mechanism for Droop Control with Virtual Inductance in a Microgrid" , Automation of Power Systems, vol. 36, no. 7, **(2012)**, pp. 27-32.
[11] K. Brabandere, B. Bolsens, J. Keybus, A. Woyte, J, Driesen and R. Belmans, " A voltage and frequency droop control method for parallel inverters" , IEEE Trans on Power Electronics, vol. 22, no. 4, **(2004)**, pp. 1107-1115.
[12] J. He and Y. Li, " Analysis, design, and implementation of virtual impedance for power electronics interfaced distributed generation" , IEEE Trans on Industrial Applications, vol. 47, no. 6, **(2011)**, pp. 2525-2538.
[13] A. Tuladhar, H. Jin, T. Unger and K. Mauch, " Control of parallel inverters in distributed AC power systems with consideration of line impedance effect" , IEEE Trans on Industrial Application, vol. 36, no. 1, **(2000)**, pp. 131-138.
[14] X. Chen, Q. Ji and F. Liu, " Smooth Transferring Control Method of Microgrids Based on Master-Slave Configuration" , Transactions of China Electrotechnical Society, vol. 29, no. 2, **(2014)**, pp. 163-170.

[15] C. Wang, Z. Xiao and S. Wang, " Synthetical control and analysis of microgrid" , Automation of Power Systems, vol. 32, no. 7, **(2008)**, pp. 98-103.
[16] M. Savaghebi, A. Jalilian, J. C. Vasquez and J. M. Guerrero, " Secondary control for voltage quality enhancement in microgrids" , IEEE Trans on Smart Grid, vol. 3, no. 4, **(2012)**, pp. 1893-1902.

Authors

Lianqing Zheng, he received his B.S. and M.S. degree in automation from Chongqing University, China, in 1987 and 1990, respectively, and his Ph.D. degrees in Mechanical Engineering from Chongqing University, China, in 2005. He has been a professor in Department of Electrical Engineering, Chongqing University, China. His research interests include power electronics, microgrid control operation, and power conversion for renewable energy.

Chen Zhuang, he received his B.S. degree in Electrical Engineering in 2012 from Chongqing University, China, where he is currently working toward the M.S. degree. His research interests include DC-AC power converter, microgrid control operation, and power conversion for renewable energy.

